American Industrial Hygiene Association Journal

ISSN: 0002-8894 (Print) (Online) Journal homepage: https://www.tandfonline.com/loi/aiha20

A comparative study of aerosol deposition in different lung models

C.P. YU & C.K. DIU

To cite this article: C.P. YU & C.K. DIU (1982) A comparative study of aerosol deposition in different lung models, American Industrial Hygiene Association Journal, 43:1, 54-65, DOI: 10.1080/15298668291410891

To link to this article: https://doi.org/10.1080/15298668291410891

Theoretical calculations are made on total and regional deposition of inhaled particles in the human respiratory system based upon various current lung models. It is found that although total deposition does not vary appreciably from model to model, considerably large differences are present in regional deposition. Deposition profiles along the airways from different models also show very different patterns. These differences can be explained in terms of airway dimensions and the number of structures in different models. Extension to explain intersubject variability is also made.

A comparative study of aerosol deposition in different lung models*

C.P. YU and C.K. DIU
Faculty of Engineering and Applied Sciences, State University of New York at Buffalo, Amherst, NY 14260

introduction

It has been well recognized that the deposition of inhaled particles in the human lung depends upon the anatomic structure and physical dimensions of the airways. Earlier theoretical investigations of particle deposition were based upon simplified airway models of Findeisen[1] and Landahl.[2] Calculated regional depositions by the Task Group on Lung Dynamics[3] using Findeisen's lung model have consistently overestimated alveolar deposition and underestimated tracheobronchial deposition when they are compared with the experimental data.[4] In recent years, because more accurate and detailed morphological measurements of the airways are available, several new airway models have been proposed. Although all these models have similar arrangements, they differ considerably in numbers of structures and airway dimensions. This is due partly to the use of different lung casts for measurement and partly to different airway identification schemes. In this paper, a theoretical study is made on total and regional deposition of inhaled particles in the lung based upon various current lung models. The purpose is to find how particle depositions are different in these models, and through comparisons with experimental data it is hoped that a proper airway model for deposition study can be identified.

lung models

Earlier model of the airways by Findeisen (Table I) consists of only a few generations. Starting with the trachea, Findeisen subdivided the branching airways and the pulmonary spaces into nine sections based on a functional concept. The last section contains 5.2×10^7 alveolar sacs. A similar division of the airways was made by Landahl, with minor modification in physical dimensions.

Modern description of the airway structure was pioneered by Weibel[5] based upon detailed measurements of a lung cast. In Weibel's symmetric lung model A (Table II), the airways are assumed to be a dichotomous branching system consisting of 23 generations. Beginning from the 17th generation, increasing numbers of alveoli are present on the airway walls, and the last three generations of airways are completely covered with alveoli. Thus, the alveolar space in this model consists of all the airways in the last seven generations.

Weibel's model has been widely used in the literature for studying gas diffusion and particle deposition because of its simplicity. In a real lung, the airways are believed to be

*Presented at the American Industrial Hygiene Conference May 25 - 29, 1981, Portland, Oregon.

TABLE I
Lung Model of Findeisen Adjusted to 3000 cm³ Lung Volume

Lung Parts	Number of Airways	Length L (cm)	Diameter d (cm)	Accumulative Volume (cm³)
Trachea	1	9.479	1.12	9.36
Main Bronchi	2	5.601	.646	13.02
1st Order Bronchi	12	2.585	.345	15.90
2nd Order Bronchi	100	1.293	.172	18.91
3rd Order Bronchi	770	.431	.129	23.26
Terminal Bronchioles	5.4×10^4	.259	.052	52.58
Respiratory Bronchioles	1.1×10^5	.129	.043	73.30
Alveolar Ducts	2.6×10^7	.017	.017	177.82
Alveolar Sacs	5.2×10^7	.026	.026	3000

TABLE II
Lung Model of Weibel Adjusted to 3000 cm^3 Lung Volume

Generation Number	Number of Airways	Length L (cm)	Diameter d (cm)	Bend Angle (degree)	Accumulative Volume* (cm^3)
0	1	10.260	1.539	95.5	19.06
1	2	4.070	1.043	55.9	25.63
2	4	1.624	.710	32.8	28.63
3	8	.650	.479	19.4	29.50
4	16	1.086	.385	40.4	31.69
5	32	.915	.299	43.8	33.75
6	64	.769	.239	46.0	35.94
7	128	.650	.197	47.3	38.38
8	256	.547	.159	49.3	41.13
9	512	.462	.132	50.2	44.38
10	1024	.393	.111	50.7	48.25
11	2048	.333	.093	51.3	53.00
12	4096	.282	.081	49.8	59.13
13	8192	.231	.070	47.2	66.25
14	16 384	.197	.063	44.5	77.13
15	32 768	.171	.056	43.4	90.69
16	65 536	.141	.051	39.4	109.25
17	131 072	.121	.046		139.31
18	262 144	.100	.043		190.60
19	524 288	.085	.040		288.16
20	1 048 578	.071	.038		512.94
21	2 097 152	.060	.037		925.04
22	4 194 304	.050	.035		1694.16
23	8 388 608	.043	.035		3000

*including alveolar volume

TABLE III
Lung Model of Olson *et al.* Adjusted to 3000 cm^3 Lung Volume

Generation Number	Number of Airways	Length L (cm)	Diameter d (cm)	Bend Angle (degree)	Accumulative Volume* (cm^3)
0	1	10.707	1.606	95.5	21.69
1	2	3.765	1.160	46.5	29.65
2	4	2.703	.839	46.2	35.62
3	7	2.088	.642	46.6	39.65
4	20	1.642	.504	46.6	46.21
5	33	1.303	.402	46.5	51.67
6	88	.955	.321	42.6	58.49
7	143	.870	.268	46.6	65.48
8	232	.696	.214	46.6	70.90
9	609	.580	.178	46.6	80.51
10	986	.473	.145	46.6	88.28
11	2580	.385	.119	46.5	99.28
12	4180	.319	.098	46.5	109.34
13	6760	.253	.080	48.6	117.99
14	17 710	.224	.066	45.0	131.57
15	28 660	.176	.054	48.6	143.10
16	46 310	.145	.045	46.3	153.57
17	121 400	.071	.045		168.40
18	196,400	.071	.058		209.56
19	514 200	.089	.067		398.42
20	832 000	.089	.031		481.74
21	1 346 300	.089	.031		789.21
22	3 524 600	.071	.031		1545.97
23	5 702 900	.054	.031		3000

*including alveolar volume

asymmetric, and Weibel's model thus overestimates the number of airway structures. Models of asymmetric airways were first proposed by Horsefield and Cumming[6] based upon the measurement of the tracheobronchial tree of their lung cast. The corresponding distal airway morphology was examined by Parker *et al.*[7] However, these references did not present a complete lung model which can readily be used for deposition study. An average complete asymmetric lung

TABLE IV
Lung Model of Hansen and Ampaya Adjusted to 3000 cm^3 Lung Volume

Generation Number	Number of Airways	Length L (cm)	Diameter d (cm)	Bend Angle (degree)	Accumulative Volume* (cm^3)
0	1	10.046	1.508	95.4	17.89
1	2	3.987	1.021	55.9	24.49
2	4	1.591	.695	32.8	.26.82
3	8	.636	.469	19.4	27.21
4	16	1.063	.376	40.4	29.74
5	32	.895	.293	43.7	31.67
6	64	.753	.234	46.1	33.75
7	128	.636	.192	47.4	36.00
8	256	.536	.155	49.4	38.62
9	512	.452	.129	50.4	41.65
10	1024	.385	.109	50.5	45.29
11	1908	.327	.092	51.1	49.72
12	3555	.277	.080	49.8	55.48
13	6624	.226	.068	47.2	62.79
14	12 343	.192	.062	44.5	72.41
15	23 000	.111	.052	30.7	77.87
16	46 000	.090	.043		86.97
17	92 000	.090	.043		106.09
18	184 000	.081	.044		142.13
19	437 000	.061	.048		213.31
20	1 035 000	.047	.047		343.90
21	2 484 000	.054	.051		680.49
22	5 842 000	.040	.039		1161.80
23	8 602 000	.038	.036		1863.36
24	8 418 000	.028	.029		2620.45
25	3 358 000	.026	.027		2884.59
26	1 333 400	.020	.024		3000

*including alveolar volume

TABLE V
Lung Model of Yeh and Schum Adjusted to 3000 cm^3 Lung Volume

Generation Number	Number of Airways	Length L (cm)	Diameter d (cm)	Bend Angle (degree)	Branching Angle $\theta°$	Gravity Angle $\phi°$	Accumulative Volume* (cm^3)
0	1	8.139	1.636	71.3	0	0	17.11
1	2	3.549	1.270	40.0	33	20	26.10
2	4	1.449	.920	22.6	34	31	29.95
3	8	.785	.673	16.7	22	43	32.18
4	16	.810	.530	21.9	20	39	35.04
5	32	.822	.467	25.2	18	39	39.55
6	64	.724	.354	29.3	19	40	44.11
7	128	.783	.304	36.9	22	36	51.37
8	256	.706	.262	38.6	28	39	61.11
9	512	.543	.209	37.2	22	45	70.67
10	1024	.453	.161	40.2	33	43	80.12
11	2048	.363	.127	41.0	34	45	89.53
12	4096	.292	.096	43.6	37	45	98.20
13	8192	.224	.075	42.8	39	60	106.28
14	16 384	.173	.059	41.6	39	60	114.12
15	32 768	.137	.049	40.1	51	60	122.51
16	65 536	.109	.044	35.5	45	60	133.35
17	131 072	.098	.041		45	60	154.21
18	262 144	.075	.038		45	60	190.78
19	524 288	.065	.037		45	60	268.78
20	1 048 576	.057	.036		45	60	476.08
21	2 097 152	.051	.036		45	60	875.12
22	4 194 304	.046	.035		45	60	1650.79
23	8 388 608	.043	.035		45	60	3000

*including alveolar volume

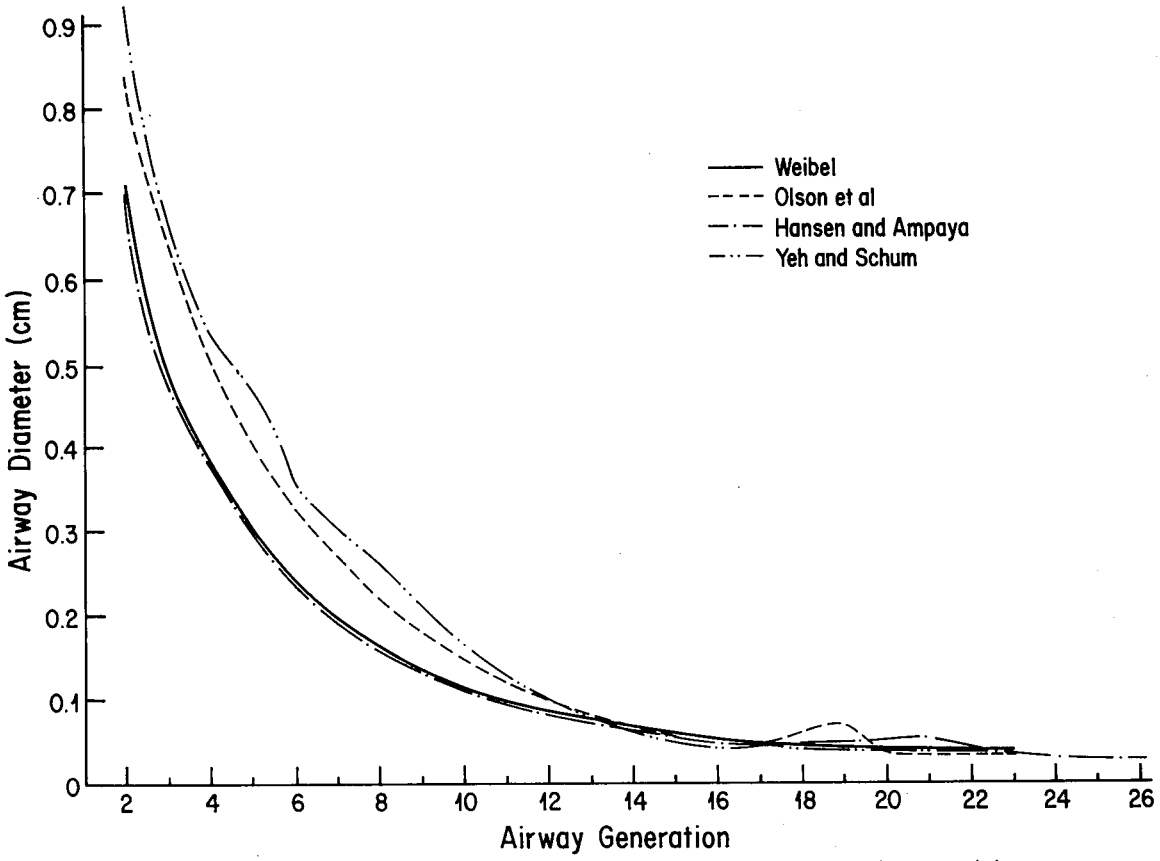

Figure 1 — Airway diameters versus airway generation for different lung models.

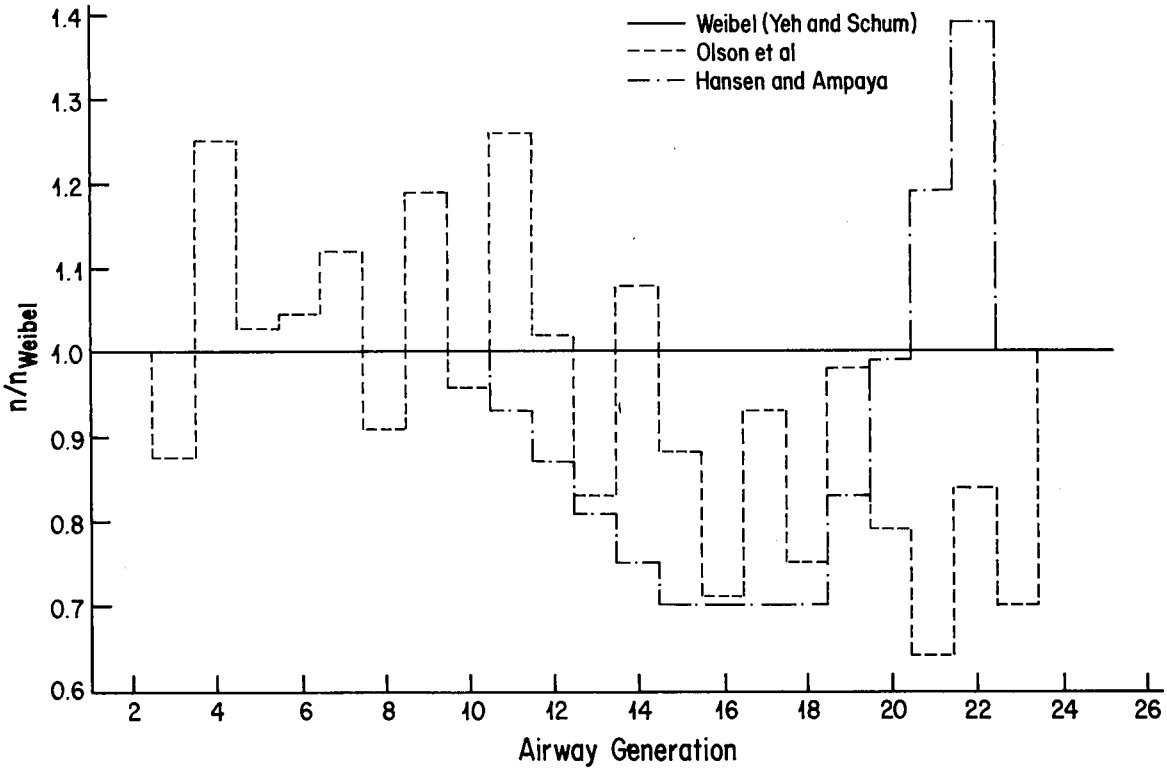

Figure 2 — Degree of asymmetry of different lung models. n denotes the number of structures at a particular generation.

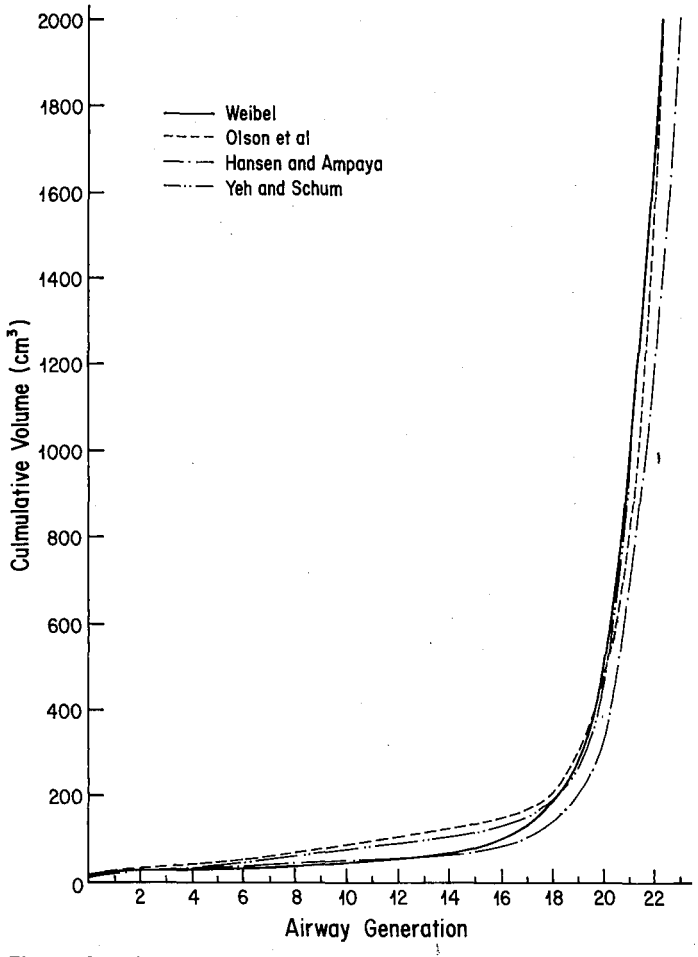

Figure 3 — Cumulative lung volume versus airway generation for different lung models. The dead space volume in Hansen and Ampaya's model is the volume from generation 0 to 15, while in the other models, this volume is from generation 0 to 16.

model, compatible with these measurements, has been proposed by Olson *et al.*,[8] as set forth in Table III. Olson's model resembles closely the model of Weibel. The numbers of airways at high orders are, however, considerably less.

Hansen and Ampaya[9] have performed a study of human parenchyma by a three dimensional enlarged reconstructed human acinus. They demonstrated a greater increase in the respiratory bronchiolar and ductual cross-sectional area and alveolar surface area in comparison to Weibel's model. By using Weibel's data for the first 10 generations of the airways and their data for generations 15-26, the diameter and length of the airways for all generations can fit smoothly into two simple mathematical equations. Table IV presents the data of this model. Again, fewer airway structures than Weibel's at high order airways are found.

More recently, Yeh and Schum[10] presented an airway model for each lobe of the lung from the measurements of a different cast. Their data include the branching angle and the angle of inclination with gravity at each airway generation. The average data of the airways for the whole lung are listed in Table V. The number of airways at each generation, however, follows the same dichotomous model.

In our calculation, we have adopted those lung models from Weibel, Olson, Hansen and Ampaya, and Yeh and Schum. A comparison of their structural differences was made by scaling their original data to an initial lung volume of 3000 cm^3. Figures 1 through 3 show, respectively, the comparison of airway diameter, number of airways, and cumulative volume versus airway generation based upon the data given in Tables II to V. The cross-sectional area versus the distance from the trachea for all models is also shown in Figure 4. It is seen that the model of Olson *et al.* has the largest airway depth, largest dead space volume and the fewest and smallest airways beyond the 20th generation,

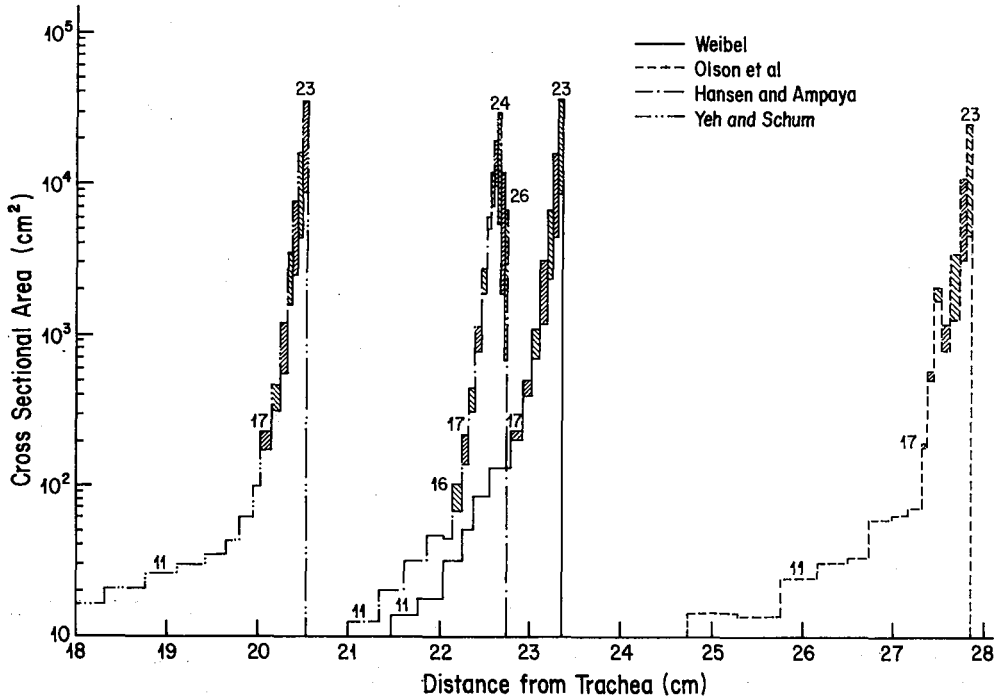

Figure 4 — Cross-sectional area as a function of the distance from the trachea for different lung models.

while a corresponding opposite situation occurs in Hansen and Ampaya's model.

mathematical deposition model

The deposition model used for present calculation is the one that we developed previously.[11] The model treats the airways as a one-dimensional distributed system in which the airway depth or the generation number is used as an independent variable. This formulation enables us to express the combined deposition efficiency in a simple form, *i.e.* the combined deposition efficiency is the algebraic sum of all individual deposition efficiencies. In addition, the model takes into account airway expansion and contraction during breathing in a natural manner, and it offers a simple mathematical solution for calculating deposition.

It has been shown before that our model provides satisfactory deposition predictions at all flow rates and particle sizes. For better comparison with experimental data, we have included in the model several additional refinements. First, new empirical deposition efficiencies in the nose and mouth are introduced. These formulae were derived from a comprehensive analysis of recent experimental data of head deposition[12] and therefore are more reliable than the previous nasal deposition expression of the Task Group on Lung Dynamics. For inspiration, the nasal deposition efficiency has the form

$$\eta_{NI} = -0.014 + 0.023 \log \frac{\rho d_p^2 Q}{(g\ \mu m^2 sec^{-1})} \qquad (1a)$$

for $\rho d^2 Q < 337\ g\ \mu m^2 sec^{-1}$

and

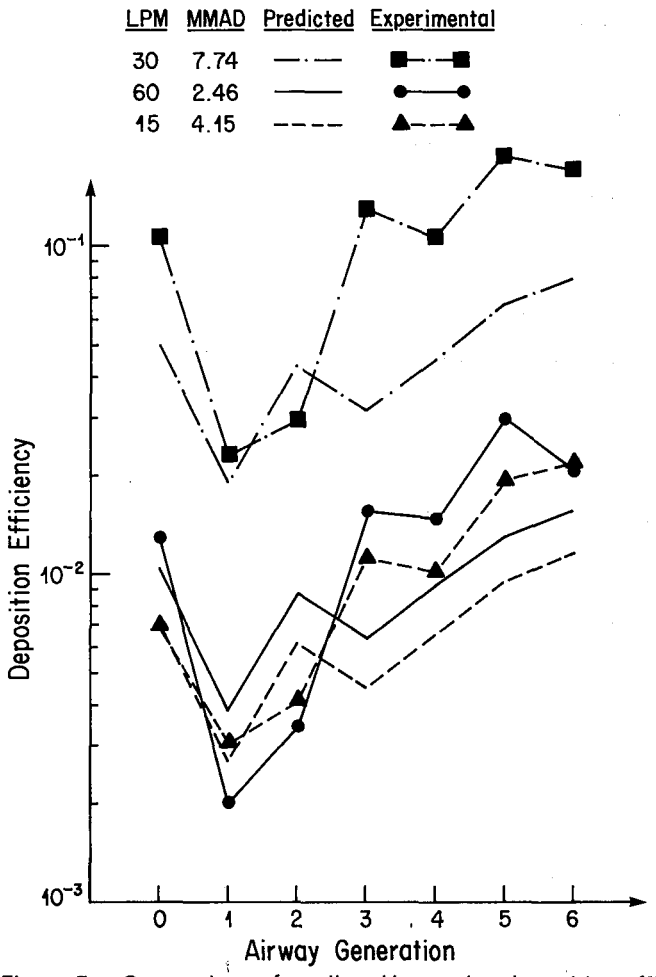

Figure 5 — Comparison of predicted impaction deposition efficiencies with experimental data of Schlesinger, *et al.*[14]

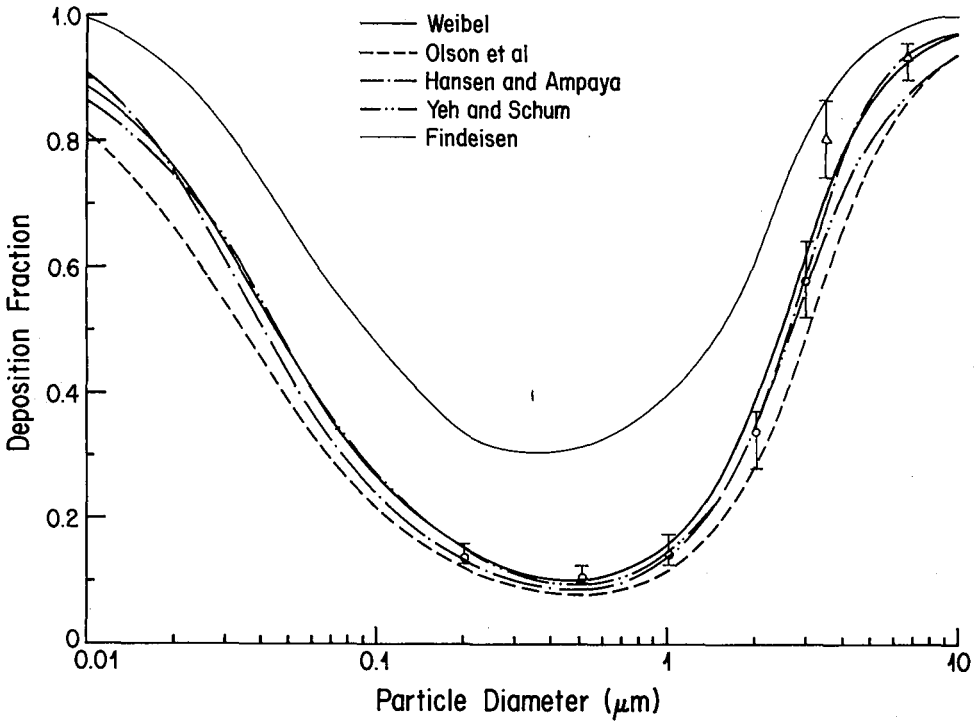

Figure 6 — Total deposition fraction for mouth-breathing calculated from different lung models. Experimental points are from Heyder, *et al.*,[17] O for 5 subjects and Foord, *et al.*,[16] Δ for 6 subjects. All experiments were performed at 1000 cm^3 tidal volume and 15 resp/min. with equal period for inspiration and expiration and no pause.

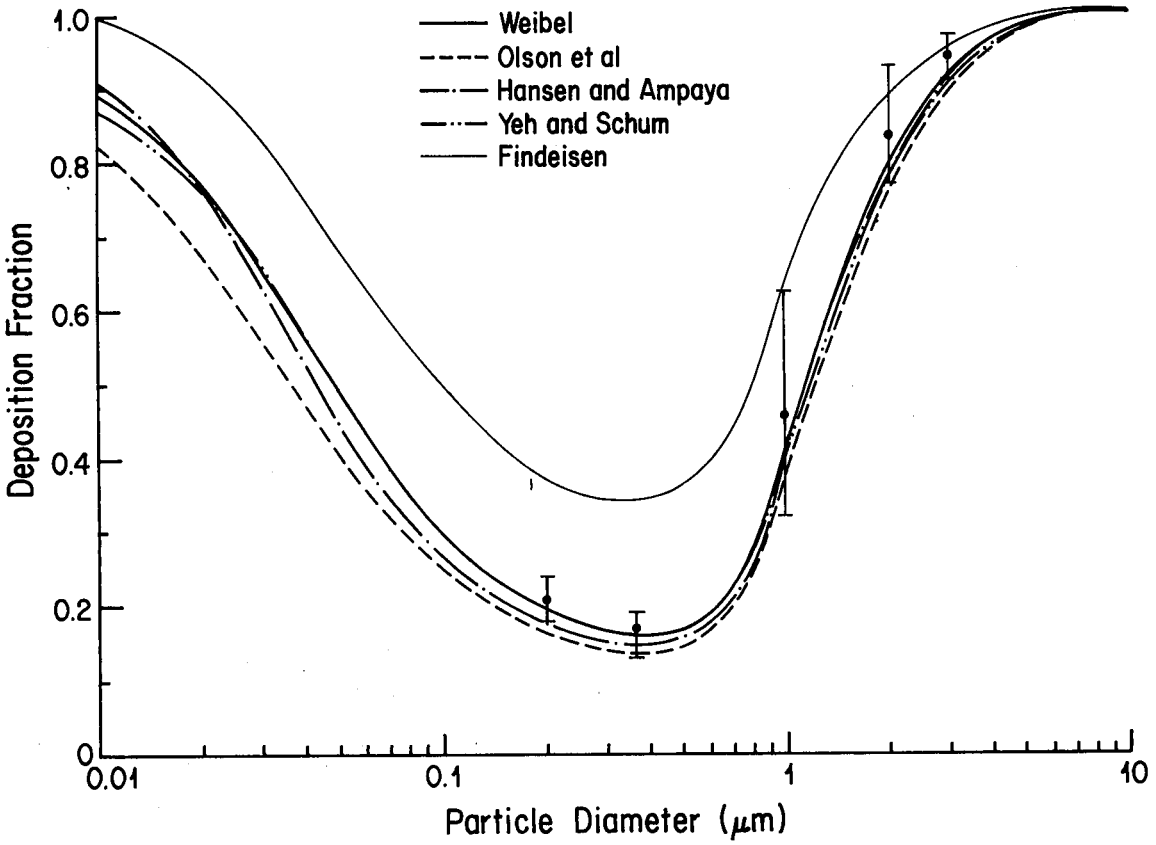

Figure 7 — Total deposition fraction for nose-breathing calculated from different lung models. Experimental points are from Heyder, *et al.*[17] for 4 subjects with the same experimental conditions as Figure 6.

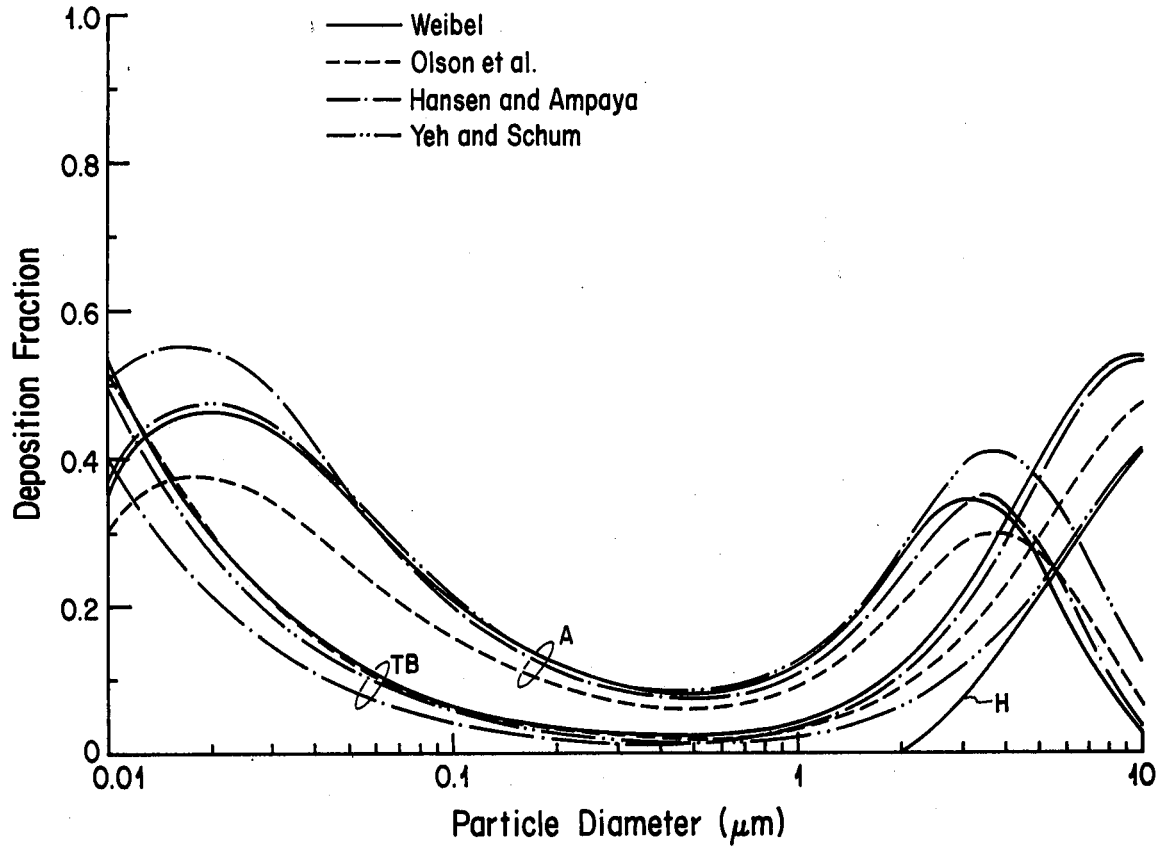

Figure 8 — Regional deposition fraction for mouth-breathing calculated from different lung models. A represents alveolar deposition, TB tracheobronchial deposition and H head deposition.

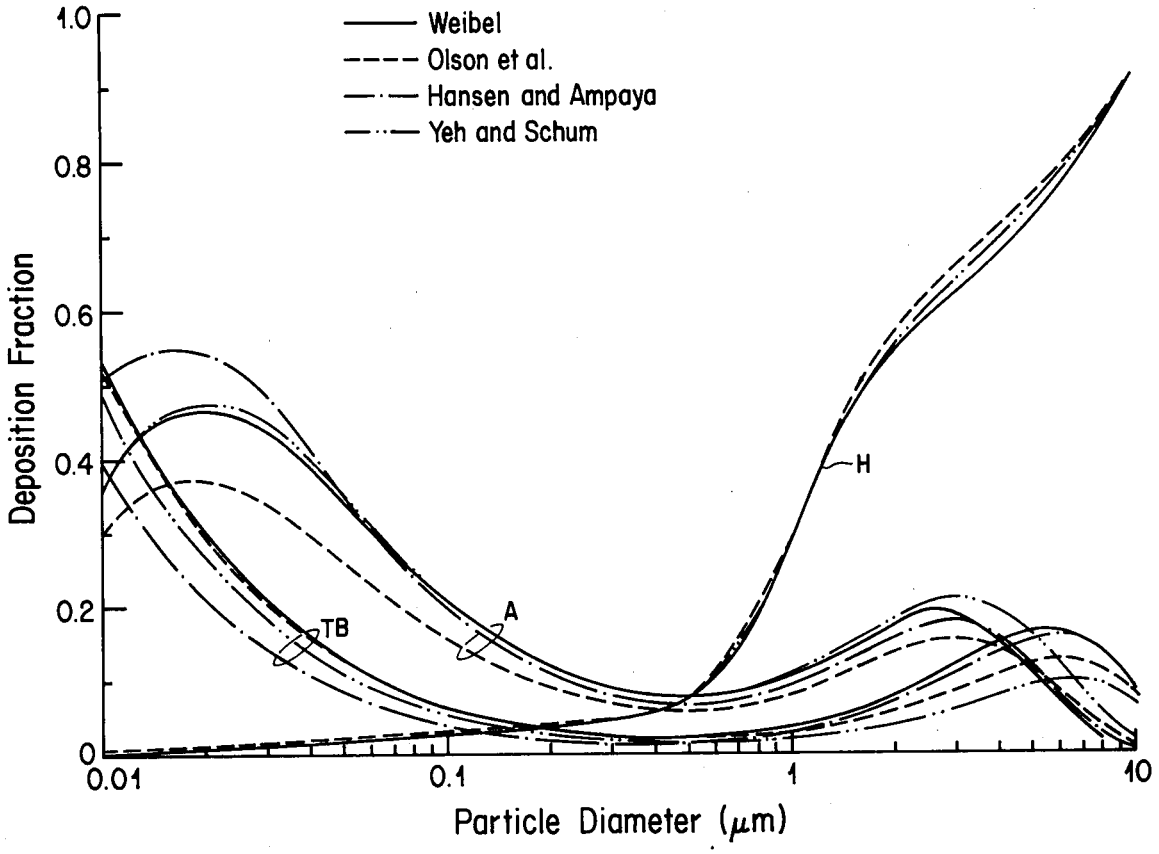

Figure 9 — Regional Deposition fraction for nose-breathing calculated from different lung models.

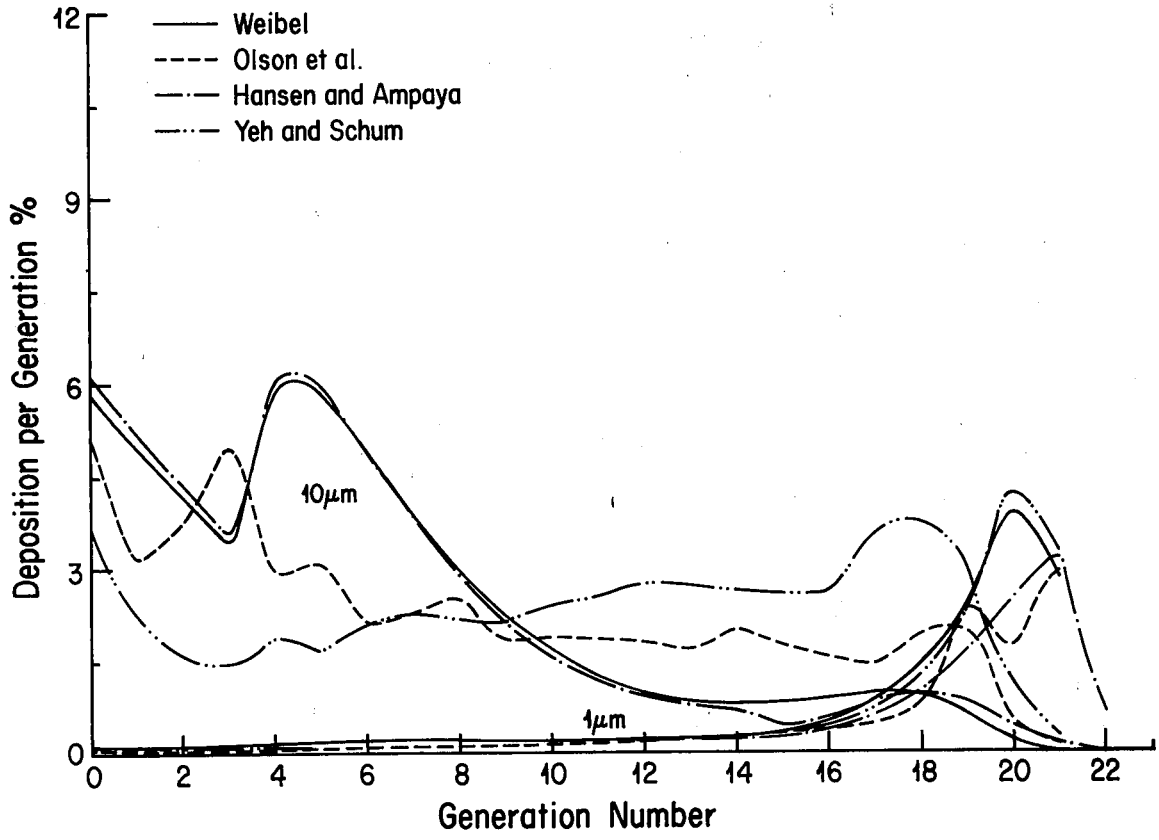

Figure 10 — Deposition profiles at mouth-breathing along airway generation for different lung models at two different particle sizes representing impaction dominated (d_p = 10 μm) and sedimentation dominated (d_p = 1 μm) region.

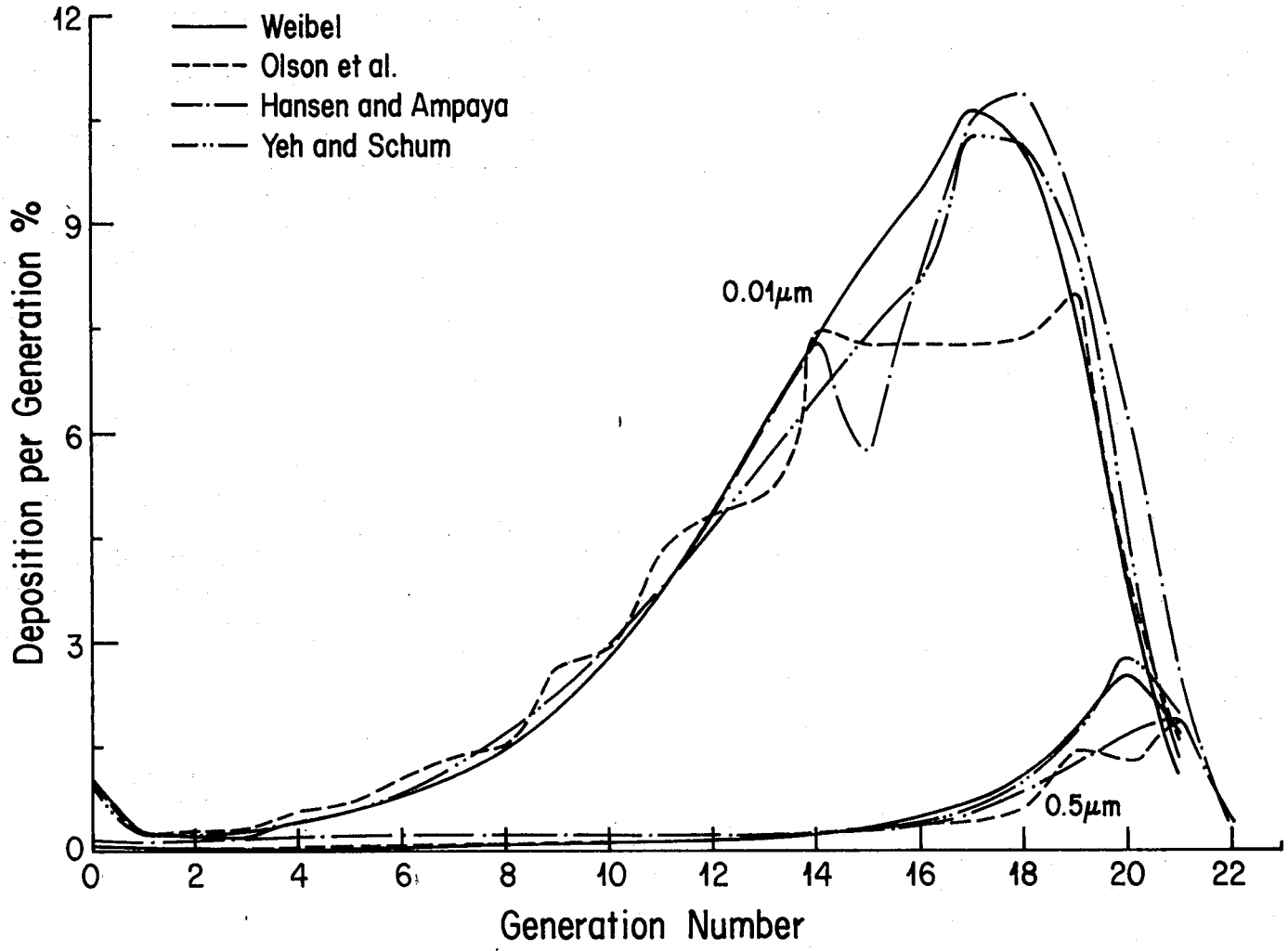

Figure 11 — Deposition profiles at mouth-breathing along airway generation for different lung models for $d_p = 0.5\ \mu m$ and diffusion dominated particle size ($d_p = 0.01\ \mu m$).

$$\eta_{NI} = -0.959 + 0.397 \log \frac{\rho d_p^2 Q}{(g\ \mu m^2 sec^{-1})} \qquad (1b)$$

for $\rho d_p^2 Q > 337\ g\ \mu m^2 sec^{-1}$

where ρ is the particle mass density, d_p the particle diameter and Q the air flow rate. For expiration, the nasal efficiency is

$$\eta_{NE} = 0.033 + 0.003 \log \frac{\rho d_p^2 Q}{(g\ \mu m^2 sec^{-1})} \qquad (2a)$$

for $\rho d_p^2 Q < 215\ g\ \mu m^2 sec^{-1}$

and

$$\eta_{NE} = -0.851 + 0.399 \log \frac{\rho d_p^2 Q}{(g\ \mu m^2 sec^{-1})} \qquad (2b)$$

for $\rho d_p^2 Q > 215\ g\ \mu m^2 sec^{-1}$

Also, the inspiratory mouth efficiency is in the form

$$\eta_{MI} = -1.117 + 0.324 \log \frac{\rho d_p^2 Q}{(g\ \mu m^2 sec^{-1})} \qquad (3a)$$

for $\rho d_p^2 Q > 3000\ g\ \mu m^2 sec^{-1}$

and

$$\eta_{MI} = 0 \qquad (3b)$$

for $\rho d_p^2 Q < 3000\ g\ \mu m^2 sec^{-1}$

and the expiratory efficiency through the mouth is assumed to be zero.

In the tracheobronchial tree, a different impaction deposition formula is adopted to replace the empirical formula which we derived previously. We assume each airway to be a bend, with the bend angle θ equal to

$$\theta = \frac{L}{4d} \qquad (4)$$

where L and d are respectively the length and diameter of the airway, and 4d is the radius of the bend. Using the impaction efficiency for a bend, we obtain[13]

$$\eta_i = 0.768\ \theta\ (St) \quad \text{for} \quad St \ll 1 \qquad (5)$$

where $St = \rho d_p^2 u/(9\ \mu d)$ is the Stokes number (ρ and d_p being particle mass density and diameter respectively, μ the fluid viscosity, d the airway diameter and u the axial fluid velocity). Figure 5 is a comparison of the calculated efficiency from Equation (5) for different airway generations with the

experimental data from a cast measurement by Schlesinger *et al.*[14] Good agreement is found for all particle sizes and flow rates.

Other minor revisions in the model include the use of turbulent diffusion deposition formula when Reynolds number exceeds 2000, and an explicit correction of sedimentation deposition due to the orientation angles of the airways. The deposition formulae used in the model are summarized in the Appendix.

deposition results and discussion

For inter-model comparisons, monodisperse aerosol with unit mass density, identical initial lung volume (or Functional Residual Capacity) and the same breathing pattern have to be used. For this purpose, we have chosen the initial lung volume to be 3000 cm^3, tidal volume to be 1000 cm^3 and breathing frequency to be 15 cycles/min. The breathing cycle consists of equal time period for inspiration and expiration with no respiratory pause. This corresponds to a control breathing pattern used frequently in many experiments.[15-17]

The dimensions of the airways for different lung models for deposition calculation are scaled to a volume of 3500 cm^3 corresponding to the initial lung volume plus one-half of the tidal volume. The scaling law for any linear dimension is assumed to follow one-third power of the lung volume.

Figures 6 and 7 show total deposition versus particle size at nose and mouth breathing calculated from the lung models of Weibel, Olson *et al.*, Hansen and Ampaya, and Yeh and Schum. A few experimental data points[16,17] are also shown there for comparison, since these data were obtained from the control breathing experiments under the same breathing condition. It is seen from these figures that the deposition curves for all current lung models do not differ greatly from each other, and they all compare reasonably well with the experimental data. The results calculated from Findeisen's model shown there, however, are consistently higher for all particle sizes. For $d_p > 0.5$ μm, deposition differences for different lung models are less for nose-breathing than that for mouth-breathing as more particles are captured in the head region.

Regional depositions are shown in Figures 8 and 9 for all lung models. Differences in deposition in this case are considerably larger than that in total deposition. For $d_p < 0.5$ μm where diffusion mechanism dominates, these differences may reach up to 17%. The model of Hansen and Ampaya exhibits the lowest tracheobronchial deposition and the corresponding highest pulmonary deposition. It is due to the smallest dead space volume and shorter path length which compensate for its smallest tracheobronchial diameters when compared to other models. On the contrary, it has the largest aerosol volume penetrating into the pulmonary region where pulmonary airway diameters are about the same as other models. It is noticed also that the model of Olson *et al.* gives the lowest pulmonary deposition with the corresponding high tracheobronchial deposition. Despite its relatively large tracheobronchial diameters, the dead space volume is the largest and thus smallest aerosol volume penetrating to the pulmonary region with the longest distance from the trachea.

For 0.5 μm $< d_p < 2.5$ μm, sedimentation dominates. The model of Yeh and Schum has the least tracheobronchial deposition and the highest pulmonary deposition. It is caused by the largest tracheobronchial diameters, smaller dead space and the shortest airway pathway. Olson's model again gives the lowest pulmonary deposition with a medium-high tracheobronchial deposition which can be explained as before.

For $d_p > 2.5$ μm, impaction deposition becomes increasingly dominant. Depositions in the nose or mouth and in the tracheobronchial region increase rapidly as the particle size increases. This results in a decline of alveolar deposition for very large particles. It is seen from the deposition curves that the model of Yeh and Schum in this particle size range continues to give the lowest tracheobronchial deposition and the highest pulmonary deposition. However, the model of Olson *et al.* has larger airway diameters in the tracheobronchial region than those in the models of Weibel and Hansen and Ampaya. Thus, alveolar deposition in Olson's model becomes larger for $d_p > 5$ μm.

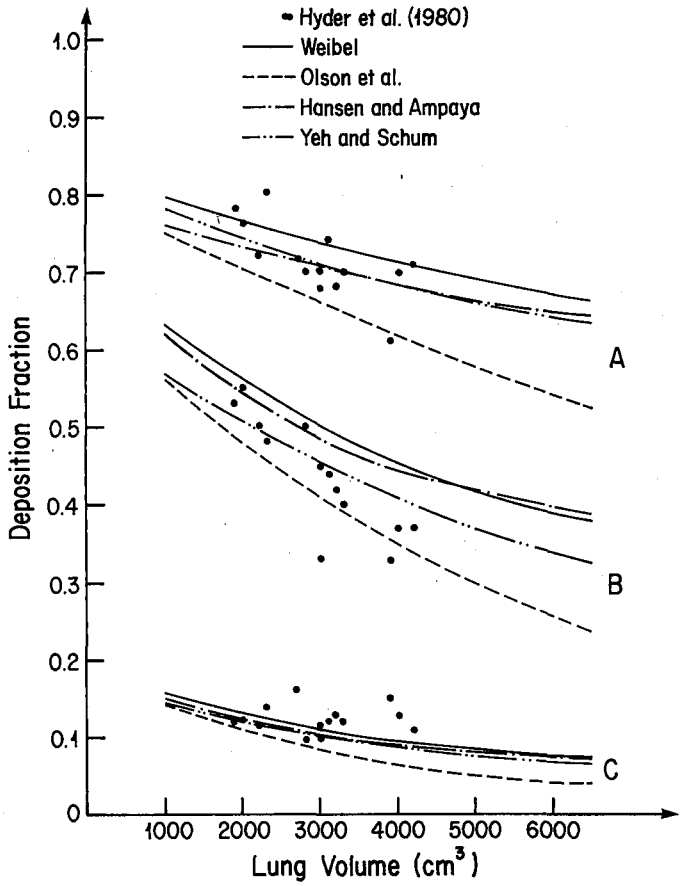

Figure 12 — Total deposition fraction versus initial lung volume for different particle sizes and breathing patterns. (A) $d_p = 2.7$ μm, $Q = 250$ cm^3/sec and T.V. $= 1500$ cm^3, (B) $d_p = 2.7$ μm, $Q = 500$ cm^3/sec and T.V. $= 1000$ cm^3, and (C) $d_p = 0.7$ μm, $Q = 500$ cm^3/sec and T.V. $= 1000$ cm^3. The breathing cycles consist of equal period for inspiration and expiration with no pause. The experimental data are by Heyder *et al.*[18] for 14 subjects.

In Figures 10 and 11, deposition profiles along airway generation are plotted for different lung models when particles of various sizes are inhaled through the mouth. These profiles are seen to have very different patterns for different lung models, particularly for 10 μm particles. Figure 10 shows the deposition profiles for impactional and sedimentational particles. Again, the highest pulmonary deposition associated with Yeh and Schum's model and that of the lowest with the model of Olson *et al.* are depicted clearly. Figure 11 shows the deposition profiles for diffusional particles. It exhibits clearly the large structural differences among these various lung models. In conclusion, these lung models used in our studies are developed from different lung casts and measurement schemes. They reflect to a certain extent intersubject variability of the human lung morphology. Thus the differences in deposition from various lung models can be used to explain the observed intersubject deposition variability under the same breathing condition. To support our argument, we calculate total deposition versus different initial lung volume with different breathing conditions as shown in Figure 12. The experiment data are from Hyder *et al.*[18] using 14 subjects. The deposition variations agree well with the differences in deposition calculated from various lung models. It is also seen in Figure 12 that Olson's lung model gives the strongest deposition dependence on the lung volume. This is due to it having the least number of structures in the pulmonary region. Consequently, the expansion of airways are the largest among all models when the lung volume is increased. The opposite situation is observed for Hansen and Ampaya's model.

acknowledgment

This work was supported by Grant No. ES-02565 from the National Institute of Environmental Health Sciences and from Grant No. OH-00923 from the National Institute for Safety and Occupational Health.

references

1. **Findeisen, W.:** Über das Absetzen kleiner, in der Luft suspendierten Teilchen in der menschlichen Lunge bei der Atmung. *Arch. Ges. Physiol. 236*:367-379 (1935).
2. **Landahl, H.D.:** On the Removal of Airborne Droplets by the Human Respiratory Tract. 1. The Lung. *Bull. Math. Biophys. 12*:43-56 (1950).
3. **Task Group on Lung Dynamics:** Deposition and Retention Models for Internal Dosimetry of the Human Respiratory Tract. *Health Phys. 12*:173-207 (1966).
4. **Mercer, T.T.:** The Deposition Model of the Task Group on Lung Dynamics: A Comparison with Recent Experimental Data. *Health Phys. 29*:673-680 (1975).
5. **Weibel, E.R.:** *Morphometry of Human Lung.* New York Academic Press (1963).
6. **Horsefield, K. and G. Cumming:** Morphology of the Bronchial Tree in Man. *J. Appl. Physiol. 24*:373-383 (1968).
7. **Parker, H., K. Horsefield and G. Cumming:** Morphology of Distal Airways in the Human Lung. *J. Appl. Physiol. 31*:386-391 (1971).
8. **Olson, D.E., G.A. Dart and G.F. Filley:** Pressure Drop and Fluid Flow Regime of Air Inspired into the Human Lung. *J. Appl. Physiol. 28*:482-494 (1970).
9. **Hansen, J.E. and E.P. Ampaya:** Human Air Space, Shapes, Sizes, Areas and Volumes. *J. Appl. Physiol. 38*:990-995 (1975).
10. **Yeh, H. and G.M. Schum:** Models of Human Lung Airways and Their Application to Inhaled Particle Deposition. *Bull. Math. Biol. 42*:461-480 (1980).
11. **Yu, C.P.:** Exact Analysis of Aerosol Deposition during Steady Breathing. *Powder Technology. 21*:55-62 (1978).
12. **Yu, C.P., C.K. Diu and T.T. Soong:** Statistical Analysis of Aerosol Deposition in Nose and Mouth. *Am. Ind. Hyg. Assoc. J. 42*:726-733 (1981).
13. **Diu, C.K. and C.P. Yu:** Deposition from Charged Aerosol Flows through a Pipe Bend. *J. Aerosol Sci. 11*:391-396 (1980).
14. **Schlesinger, R.B., D.E. Bohning, T.L. Chan and M. Lippmann:** Particle Deposition in a Hollow Cast of the Human Tracheobronchial Tree. *J. Aerosol Sci. 8*:429-445 (1977).
15. **Heyder, J., J. Gebhart, G. Heigwer, C. Roth and W. Stahlhofen:** Experimental Studies of the Total Deposition of Aerosol Particles in the Human Respiratory Tract. *J. Aerosol Sci. 4*:191-208 (1973).
16. **Foord, N., A. Black and M. Walsh:** Regional Deposition of 2.5 - 7.5 μ Dia. Inhaled Particles in Healthy Non-smokers. *J. Aerosol Sci. 9*:343-357 (1978).
17. **Heyder, J., L. Armbruster, J. Gebhart, E. Grein and W. Stahlhofen:** Total Deposition of Aerosol Particles in the Human Respiratory Tract for Nose and Mouth Breathing. *J. Aerosol Sci. 6*:311-328 (1975).
18. **Heyder, J., J. Gebhart and W. Stahlhofen:** (Ch. 3) Inhalation of Aerosols: Particle Deposition and Retention. In *Generation of Aerosols and Facilities for Exposure Experiments.* K. Willeke, Ed., Ann Arbor Science (1980).

APPENDIX

Deposition Efficiencies per Airway Generation

1. Impaction

$$\eta_i = 0.768\,\theta\,(St) \qquad \text{(A-1)}$$

where

$$St = \frac{\rho d_p^2 u}{9\,\mu d}$$

and

$$\theta = \frac{L}{4d} = \text{bend angle}$$

in which

ρ = mass density of the particle
d_p = diameter of the particle
u = mean flow velocity
μ = air viscosity
d = diameter of the airway
L = length of the airway

2. Sedimentation

$$\eta_s = \frac{2}{\pi}\left[2\epsilon\sqrt{1-\epsilon^{2/3}} - \epsilon^{1/3}\sqrt{1-\epsilon^{2/3}} + \sin^{-1}\epsilon^{1/3}\right] \quad \textbf{(A-2)}$$

where

$$\epsilon = \frac{3u_s L}{4\,ud}\sin\phi$$

in which

u_s = settling velocity of the particle
ϕ = angle of inclination of the airway to the vertical

In the present calculation for all lung models, we have used $\sin\phi = \pi/4$ which corresponds to the case of a system of randomly orientated airways. The use of tabulated values of ϕ from the model of Yeh and Schum in the calculation gives very small effect.

3. Diffusion

(i) Turbulent Flow

$$\eta_{td} = 4.0\,\Delta^{1/2}(1 - 0.444\,\Delta^{1/2} + \ldots) \quad \textbf{(A-3)}$$

(ii) Laminar Flow

$$\eta_d = 1 - 0.819e^{-14.63\Delta} - 0.0976e^{-89.22\Delta} - 0.0325e^{-228\Delta} - 0.0509e^{-125.9\Delta^{2/3}} \quad \textbf{(A-4)}$$

where

$$\Delta = \frac{DL}{d^2u}$$

in which

D = Diffusion coefficient of the particle